

MOBODY: Model Based Off-Dynamics Offline Reinforcement Learning

Yihong Guo^{*} Yu Yang[†] Pan Xu[‡] Anqi Liu[§]

Abstract

We study the off-dynamics offline reinforcement learning (RL) problem, where the goal is to learn a policy from offline datasets collected from source and target domains with mismatched transition dynamics. Existing off-dynamics offline RL methods typically either filter source transitions that resemble those of the target domain or apply reward augmentation to source data, both constrained by the limited transitions available from the target domain. As a result, the learned policy is unable to *explore* target domain beyond the offline datasets. We propose MOBODY, a Model-Based Off-Dynamics offline RL algorithm that addresses this limitation by enabling exploration of the target domain via learned dynamics. MOBODY generates new synthetic transitions in the target domain through model rollouts, which are used as data augmentation during offline policy learning. Unlike existing model-based methods that learn dynamics from a single domain, MOBODY tackles the challenge of mismatched dynamics by leveraging both source and target datasets. Directly merging these datasets can bias the learned model toward source dynamics. Instead, MOBODY learns target dynamics by discovering a *shared latent representation* of states and transitions across domains through representation learning. To stabilize training, MOBODY incorporates a behavior cloning loss that regularizes the policy. Specifically, we introduce a *Q-weighted behavior cloning loss* that regularizes the policy toward actions with high target-domain Q-values, rather than uniformly imitating all actions in the dataset. These Q-values are learned from an enhanced target dataset composed of offline target data, augmented source data, and rollout data from the learned target dynamics. We evaluate MOBODY on standard MuJoCo benchmarks and show that it significantly outperforms state-of-the-art baselines, with especially pronounced improvements in challenging scenarios where existing methods struggle.

1 Introduction

Reinforcement learning (RL) (Kaelbling et al., 1996; Li, 2017) aims to learn a policy that maximizes cumulative reward by interacting with an environment and collecting the corresponding rewards. While RL has led to impressive successes in many domains, real-world applications, such as autonomous driving (Kiran et al., 2021) and healthcare (Lee et al., 2023), face significant constraints on interaction with the environment due to safety or cost concerns. One solution is to learn a policy

^{*}Johns Hopkins University; email: yguo80@jhu.edu

[†]Duke University; email: yu.yang@duke.edu

[‡]Duke University; email: pan.xu@duke.edu

[§]Johns Hopkins University; email: aliu.cs@jhu.edu

from a pre-collected offline dataset (Levine et al., 2020). Still, when the offline dataset is insufficient, data from another environment, such as a simulator with potentially mismatched dynamics, may be needed but requires further domain adaptation. In our paper, we study a specific type of domain adaptation in RL, called off-dynamics offline RL (Liu et al., 2022, 2024a; Lyu et al., 2024b), where the simulator (source) and real/deployed (target) environments differ in their transition. The agent is not allowed to interact with the environment but only has access to offline data that are pre-collected from the two domains with mismatched dynamics and trains a policy with the offline data. Existing works on off-dynamics offline RL solve the problem by 1) reward shaping that accounts for the dynamics shift (Liu et al., 2022; Wang et al., 2024; Lyu et al., 2024a) or 2) filtering the source transition that is similar to the target transition (Xu et al., 2023; Wen et al., 2024; Liu et al., 2024a). All of them are model-free methods which lack the *exploration* in the target domain and thus might theoretically be unable to find the optimal policy if the offline dataset has poor coverage of the optimal policy (Zhan et al., 2022). Model-based methods have been proven effective in both offline and online RL, which can be more sample-efficient and allow for more exploration of the environment with learned dynamics. In this paper, we propose a Model-Based Off-Dynamics RL algorithm (MOBODY) that first learns target domain dynamics and rollouts new data from the learned dynamics during policy optimization.

However, learning the target dynamics using a mixed dataset with dynamics shift is harder compared to learning dynamics for a single domain in existing model-based offline RL (Yu et al., 2020, 2021; Rigter et al., 2022). First, the target data are limited, so we cannot directly learn the target dynamics only using the target data. Second, the existing dynamics learning methods learn the dynamics for a single domain and cannot be directly applied or adapted to other domains. Though straightforwardly we can learn dynamics by directly combining the source and target data, the learned dynamics will not work for the target domain due to the dynamics mismatch. As shown in Figure 1, MOPO that directly learns dynamics with combined source and target data significantly underperforms MOBODY which is specifically optimized to learn the *target* dynamics. This justifies the need of a novel dynamics learning algorithm that learns *target* dynamics with both source data and limited target data for model-based off-dynamics RL.

The proposed MOBODY algorithm first learns a *target* dynamics with source data and limited target data, and then learns a policy with enhanced target domain data consisting of reward augmented offline source data, offline target data and rollout data from the learned dynamics. For dynamics learning, MOBODY learns shared latent representations of states and transitions respectively across domains through representation learning by novel representation encoder loss and a novel cycle transition loss, which takes advantage of the data from both source and target domains. After we learn the target dynamics, we roll out new data with the learned dynamics during the policy optimization and optimize the policy with *enhanced target data* consisting of reward

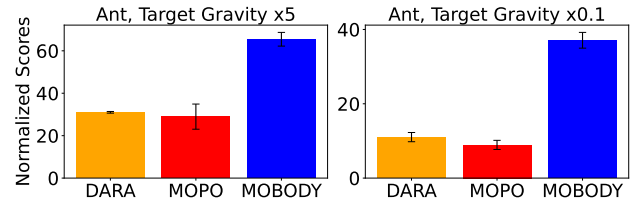


Figure 1: Comparison between DARA (Liu et al., 2022) (a model-free reward augmentation method), MOPO (Yu et al., 2020) (a vanilla model-based offline RL), and MOBODY on two MuJoCo environments with different dynamics shift type and level. We find that MOBODY substantially outperforms DARA and MOPO by exploring the *target* environment. For experiment details, see Section 5.

augmented source data, target data and new rollout data. To stabilize the policy optimization training especially when data are out of distribution, we utilize the behavior cloning loss to regularize the policy (Fujimoto and Gu, 2021). However, vanilla behavior cloning loss will push the policy to favor the action in the source data, but the action in the source data might not perform well in the target domain due to the dynamics shift. Inspired by the advantage-weighted regression (Peters and Schaal, 2007; Kostrikov et al., 2021a), MOBODY incorporates a Q-weight behavior cloning loss regularization, which will up-weight action with the high *target* Q value, while the target Q function is learned with the aforementioned *enhanced target data*.

Our contribution can be summarized as follows:

- We propose a novel paradigm for off-dynamics offline RL, called model-based off-dynamics offline RL, that can explore the target domain with the learned target transitions.
- We propose a novel framework for learning the *target* dynamics with source data and limited target data by learning a shared state representation and the transition in the latent space. For the offline RL, we learn a policy with rollout data from the learned dynamics. We also incorporate a Q-weighted behavior cloning loss for policy optimization that is simple, efficient, and more suitable to off-dynamics offline RL setting than vanilla behavior cloning loss.
- We evaluate our method on MuJoCo environments in the offline setting with different types and levels of off-dynamics shifts and demonstrate the superiority of our model with an average 58% improvement over baseline methods across all the settings.

2 Related Work

Off-dynamics RL. Off-dynamics RL aims to transfer the policy learned in the source domain to the target domain. One line of work is to augment the reward of the source data with the target data using the domain classifier. Following this idea, DARC (Eysenbach et al., 2020) and DARAIL (Guo et al., 2024) solve the off-dynamics RL problem in the online paradigm, while DARA (Liu et al., 2022) and RADT (Wang et al., 2024) use the reward augmentation techniques in the offline RL setting. Similarly, BOSA (Liu et al., 2024a) addresses the out-of-distribution problem through two support-constrained objectives. PAR (Lyu et al., 2024a) learns the representation to measure the deviation of dynamic mismatch via the state and state-action encoder to modify the reward. Another line of work is utilizing the data filter method, including the VGDF (Xu et al., 2023) and IGDF (Wen et al., 2024), which filter out the trajectories similar to the target domain and train the RL policies on filtered data. These data filtering or reward augmentation methods in off-dynamics offline RL settings cannot explore the target domain substantially, while we propose a novel model-based method that can explore the target domain with the learned *target* dynamics. There is also an active line of work that solves off-dynamics RL via learning the distributionally robust MDPs where the goal is to train a policy under the worst possible transition dynamics within an uncertainty set of the source domain (Satia and Lave Jr, 1973; Iyengar, 2005; Nilim and El Ghaoui, 2005; Xu and Mannor, 2006; Wiesemann et al., 2013). Under this robust MDP philosophy, theoretical foundations and sample efficient algorithms have been developed for both online RL (Liu and Xu, 2024a; Lu et al., 2024; Liu et al., 2024b) and offline RL (Zhou et al., 2021; Yang et al., 2022; Shi and Chi, 2024; Liu and Xu, 2024b; Tang et al., 2024), to name a few.

Model-based Offline RL. Model-based offline RL leverages the strengths of model-based methods in the offline RL paradigm. MOREL (Kidambi et al., 2020) and MOPO (Yu et al., 2020) modify reward functions based on uncertainty estimations derived from ensembles of models. VI-LCB (Rashidinejad et al., 2021) leverages pessimistic value iteration, incorporating penalty functions into value estimation to discourage poorly-covered state-action pairs. COMBO (Yu et al., 2021) provides a conservative estimation without explicitly computing uncertainty, using adversarial training to optimize conservative value estimates. RAMBO (Rigter et al., 2022) further builds upon adversarial techniques by directly training models adversarially with conservatively modified dynamics to reduce distributional shifts. These methods are designed for one domain instead of an off-dynamics RL setting. In this paper, we propose a novel dynamics learning and policy optimization method for an off-dynamics RL setting.

Representation Learning in RL. Representation learning (Botteghi et al., 2025) is actively explored in image-based reinforcement learning tasks (Zhu et al., 2020; Kostrikov et al., 2021b; Liu et al., 2021; Yarats et al., 2022) to learn the representation of the image. For model-based RL, to improve sample efficiency, representation has been widely applied to learn the latent dynamics modeling (Karl et al., 2017; Hansen et al., 2022a), latent state representation learning (Barreto et al., 2017; Fujimoto et al., 2021), or latent state-action representation learning (Ye et al., 2021; Hansen et al., 2022b; Fujimoto et al., 2023; Ota et al., 2020). In our paper, we learn the shared representation of the state and transition to auxiliary the *target* dynamics learning with source domain data.

3 Background

Off-dynamics offline reinforcement learning. We consider two Markov Decision Processes (MDPs): the source domain $\mathcal{M}_{\text{src}} = (\mathcal{S}, \mathcal{A}, R, p_{\text{src}}, \gamma)$ and the target domain $\mathcal{M}_{\text{trg}} = (\mathcal{S}, \mathcal{A}, R, p_{\text{trg}}, \gamma)$. The difference between the two domains lies in the transition dynamics p , i.e., $p_{\text{src}} \neq p_{\text{trg}}$ or more specifically, $p_{\text{src}}(s' | s, a) \neq p_{\text{trg}}(s' | s, a)$. Following existing literature on off-dynamics RL (Eysenbach et al., 2020; Liu et al., 2022; Lyu et al., 2024a; Guo et al., 2024; Lyu et al., 2024b; Wen et al., 2024), we assume that reward functions are the same across the domains, which is modeled by the state, action, and next state, i.e., $r_{\text{src}}(s, a, s') = r_{\text{trg}}(s, a, s')$. The dependency of the reward on s' is well-justified in many simulation environments and applications, such as the Ant environment in MuJoCo, where the reward is based on how far the Ant moves forward, measured by the change in its x-coordinate (i.e., the difference between the x-coordinate after and before taking action). The goal is to learn a policy π with source domain data $(s, a, s', r)_{\text{src}}$ and limited target domain data $(s, a, s', r)_{\text{trg}}$ that maximize the cumulative reward in the target domain $\max_{\pi} \mathbb{E}_{\pi, p_{\text{trg}}} [\sum_t \gamma^t r_{\text{trg}}(s, a)]$. In the offline setting, we are provided with static datasets from a source and a target domain $\mathcal{D}_{\text{src}} = \{(s, a, s', r)_{\text{src}}\}$ and $\mathcal{D}_{\text{trg}} = \{(s, a, s', r)_{\text{trg}}\}$, which consist of the transitions/trajectories collected by some unknown behavior policy. Note that in the off-dynamics setting, the number of transitions from the target domain is significantly smaller than the source, i.e., $|\mathcal{D}_{\text{trg}}| \ll |\mathcal{D}_{\text{src}}|$, and normally the ratio $\frac{|\mathcal{D}_{\text{src}}|}{|\mathcal{D}_{\text{trg}}|}$ can vary from 10 to 200. In our paper, we follow the ODRL benchmark (Lyu et al., 2024b) in which the ratio is 200.

Model-based offline reinforcement learning. Recent work in model-based RL learns a transition function $\hat{T}_{\theta}(s', r | s, a)$ by maximizing the the likelihood $\hat{T}_{\theta} = \max_{T_{\theta}} \mathbb{E}_{\mathcal{D}_{\text{offline}}} [\log \hat{T}_{\theta}(s', r | s, a)]$.

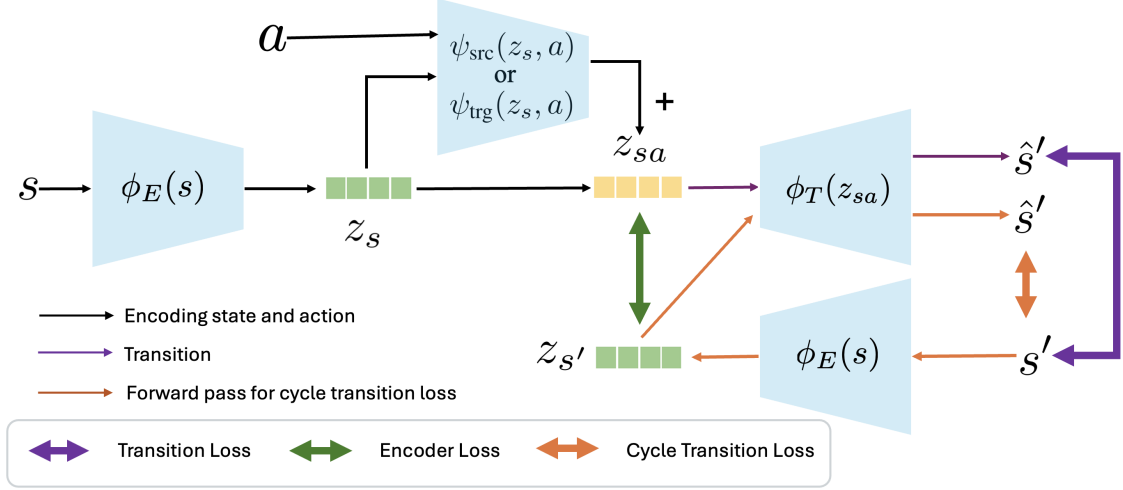


Figure 2: Architecture of the dynamics model. MOBODY encodes the state with ϕ_E and state action with ψ , outputs the next state through ϕ_T , and learns the dynamics for both domains by transition loss shown in purple double arrow \Leftrightarrow . It learns the state action representation by matching the state action representation z_{sa} with the next state representation $z_{s'}$ through encoder loss shown in the green double arrow \Leftrightarrow and the state representation through cycle transition loss shown in orange double arrow \Leftrightarrow .

Then with the learned transition, the algorithm rollout new transition data to optimize the policy and take $u(s, a)$ as the uncertainty quantification to obtain a conservative transition, i.e. $(s, a, s', \hat{r} - \beta u(s, a))$. Then they learn a policy with offline data $\mathcal{D}_{\text{offline}}$ and online rollout $(s, a, s', \hat{r} - \beta u(s, a))$. However, different from traditional model-based offline RL, we only have very limited target domain data and a source data with dynamics shift. There is no existing model-based solution for off-dynamics RL, which calls for novel methodology development both in dynamics learning and policy learning.

4 MOBODY: Model-Based Off-Dynamics Offline Reinforcement Learning

In this section, we present our algorithm, MOBODY, for the off-dynamics offline RL problem setting. We first present how we learn the *target* dynamics with very limited target domain data \mathcal{D}_{trg} and source domain data \mathcal{D}_{src} . Secondly, for policy learning, we incorporate a target Q-weighted behavior cloning loss to regularize the policy, where the target Q value is learned from *enhanced target data*, including reward augmented source data, target data, and rollout data from learned dynamics. The algorithm is summarized in Algorithm 2.

4.1 Learning the Target Dynamics

In our work, we utilize a general assumption of learning dynamics through representation learning that is widely adopted in previous literature: *the state action representation should be close to*

the next state representation in the latent space (Ye et al., 2021; Hansen et al., 2022b; Fujimoto et al., 2023). This is based on the decomposition of the dynamics in representation learning $P_\theta(s'|s, a) = \psi(s, a)^T \phi(s')$, and maximizing the likelihood with transition data, which is the product of two representation vectors, encourages the state-action representation $\psi(s, a)$ to align with the representation of the next state $\phi(s')$. This is similar to the low-rank MDPs assumptions widely used in theoretical analysis of RL (Jin et al., 2020), but we are not restricted to this as we further learn a transition to map the representation to the next state.

So, the problem becomes learning a good representation of the state, as well as learning a state action representation for the two domains to match the next state representation. We further assume that state representation and transition are shared, and state action representation is different across domains.

In general, the dynamics can be modeled as $s' = \phi_T(s, a)$. In our work, we further propose to model the state and state action representation through $z_s = \phi_E(s)$, $z_{sa}^{\text{trg}} = \psi_{\text{trg}}(z_s, a)$ and $z_{sa}^{\text{src}} = \psi_{\text{src}}(z_s, a)$, so that we can obtain a separate state action representation for two domains. So, with the learned representation z_s and z_{sa} , we have the dynamics modeled as $s' = \phi_T(z_s, \psi(z_s, a))$, where ϕ_T is the transition function. For simplicity and to reduce the model parameters, we choose to directly add the state and state action representation together and feed into the transition function $s' = \phi_T(z_s + \psi(z_s, a))$. We show the flow of dynamics learning component in Figure 2. And our dynamics learning model is:

$$\text{source dynamics : } z_s = \phi_E(s), z_{sa} = z_s + \psi_{\text{src}}(z_s, a), \hat{s}' = \phi_T(z_{sa}), \quad (4.1)$$

$$\text{target dynamics : } z_s = \phi_E(s), z_{sa} = z_s + \psi_{\text{trg}}(z_s, a), \hat{s}' = \phi_T(z_{sa}), \quad (4.2)$$

where ϕ_E is the state encoder, ϕ_T is the transition, and ψ_{src} and ψ_{trg} are the state action encoder for source and target respectively. Now we talk about how we learn the representation and dynamics.

Encoder Loss. As mentioned, to learn the representation of the model, we adopt a general assumption in representation learning that the representation of the state action should be close to the next state. The encoder loss is shown in a green two-way arrow in Figure 2.

$$L_{\text{rep}} = \frac{1}{N} \sum_{i=1}^N \| |z_{s'}|_{\times} - (z_s + \psi_{\text{src}}(z_s, a)) \|^2, \quad (4.3)$$

$z_{s'} = \phi_E(s')$ is the next state representation encoded with ϕ_E and $|\cdot|_{\times}$ is the stop gradient. We apply the stop gradient to prevent backpropagation through $z_{s'}$.

Transition Loss. The transition loss minimizes the Mean Squared Error (MSE). It is shown in a purple two-way arrow in Figure 2. The transition loss will optimize the transition function ϕ_T .

$$L_{\text{dyn}}^{\text{src}} = \frac{1}{N} \sum_{i=1}^N \| s' - \phi_T(z_s + \psi_{\text{src}}(z_s, a)) \|^2; L_{\text{dyn}}^{\text{trg}} = \frac{1}{N} \sum_{i=1}^N \| s' - \phi_T(z_s + \psi_{\text{trg}}(z_s, a)) \|^2. \quad (4.4)$$

Cycle Transition Loss. To further improve the state representation quality, we include a “cycle transition loss” through VAE-style (Kingma et al., 2013) learning. The dynamics function maps the state action to the next state through the state action representation. Then, from one perspective, by setting ψ to 0, the dynamics only input the state into the dynamics learning framework, and no

action will be taken. The output of the dynamics will be exactly the same state, i.e. $(s, 0, s)$. So when the ψ is set to 0, the state is predicted as: $\hat{s} = \phi_T(\phi_E(s) + 0)$. Then we can explicitly learn the state representation with state in the offline dataset by minimizing: $\|\phi_T(\phi_E(s)) - s\|_2$. From this perspective, we can view the ϕ_E as an encoder and ϕ_T as a decoder, and we propose to use Variational AutoEncoder (VAE) (Kingma et al., 2013) to learn state representation.

Let z_s be expressed as $z_s = \mu_{\phi_E}(s) + \sigma_{\phi_E}(s) \odot \epsilon$, with $\epsilon \sim \mathcal{N}(0, I)$ and $\mu_{\phi_E(s)}$ and σ_{ϕ_E} are the output of state encoder network ϕ_E . Let d_z be the dimension of the latent representation, the loss for learning the state representation is:

$$\mathcal{L}_{\text{cycle}} = \frac{1}{2N} \sum_{i=1}^N \sum_{j=1}^{d_z} (\mu_{i,j}^2 + \sigma_{i,j}^2 - \log \sigma_{i,j}^2 - 1) + \frac{1}{N} \sum_{i=1}^N \|s_i - \hat{s}_i\|_2, \quad (4.5)$$

The cycle transition loss is shown in an orange two-way arrow in Figure 2.

We can also interpret the cycle transition loss from another perspective. As mentioned earlier, we want to push the state-action representation to be close to the next state representation. This suggests that for the next state representation given by the state encoder $\phi_E(s')$, when input the next state representation, the encoder will also give us the next state. So, we also want to minimize the distance between the next state s' and the predicted next state $\phi_T(\phi_E(s'))$.

Reward learning Note that the reward is modeled as a function of (s, a, s') tuple, as in many tasks, the reward is also related to the next state as mentioned in Section 3. Also, recall that the reward function in the source and target domain remains the same. Thus, we can learn the reward function with source and target domain data together via the following loss function.

$$L_{\text{reward}} = \frac{1}{2} \mathbb{E}_{D_{\text{src}} \cup D_{\text{trg}}} [r(s, a, s') - \hat{r}(s, a, s')]^2 + \frac{1}{2} \mathbb{E}_{D_{\text{src}} \cup D_{\text{trg}}} [r(s, a, s') - \hat{r}(s, a, \hat{s}')]^2, \quad (4.6)$$

where \hat{s}' is the predicted next state. Here, we use both the true next state and the predicted next state from the dynamics model to learn the reward model, as during inference, we do not have the true next state and only have a predicted next state.

Then to summarize, the dynamics learning loss will be:

$$\min \mathbb{E}_{D_{\text{src}} \cup D_{\text{trg}}} L_{\text{dyn}}^{\text{src}} + L_{\text{dyn}}^{\text{trg}} + L_{\text{reward}} + \lambda(L_{\text{cycle}} + L_{\text{rep}}), \quad (4.7)$$

where λ is a scalar that controls the weight of the representation learning term. We summarize the dynamics learning algorithm in Algorithm 1.

Uncertainty quantification of the transition To capture the uncertainty of the model, we learn N ensemble transition models, with each model trained independently via Eq.(4.7). We design the uncertainty quantification of the reward estimation as $u(s, a) := \max_i \text{Std}(\hat{s}'_j) = \max_i \sqrt{1/N \sum_{j=1}^N (\hat{s}'_j - \mathbb{E}(\hat{s}'))^2}$, which is the largest standard deviation among all the state dimensions. This simple and intuitive uncertainty quantification using the ensemble model has been proven simple and effective in many machine learning literature (Parker, 2013) and also model-based RL algorithms (Yu et al., 2020). We find it sufficient to achieve good performance in our experiments by employing the penalized reward \tilde{r} for the downstream policy learning: $\tilde{r}(s, a, s') = \hat{r}(s, a, s') - \beta u(s, a)$.

Algorithm 1 Dynamics Learning via Cycle Transition Loss

- 1: **Input:** Offline datasets $\mathcal{D}_{\text{src}} = \{(s, a, r, s')\}$, $\mathcal{D}_{\text{trg}} = \{(s, a, r, s')\}$, number of model learning steps N_{model} , target training frequency K .
 - 2: **Initialize:** State encoder model ϕ_E , transition model ϕ_T , source state action encoder ψ_{src} , target state action encoder ψ_{trg} , reward model \hat{r} .
 - 3: **for** $i = 1$ to N_{model} **do**
 - 4: **Sample mini-batch:**
 - 5: **if** $i \% K = 0$ **then**
 - 6: Sample mini-batch $\{(s, a, r, s')\}$ from \mathcal{D}_{trg}
 - 7: **else**
 - 8: Sample mini-batch $\{(s, a, r, s')\}$ from \mathcal{D}_{src}
 - 9: **end if**
 - 10: Predict the next state with Equation (4.1), and Equation (4.2) with mini-batch data.
 - 11: Optimize the dynamics with the loss in Equation (4.7)
 - 12: **end for**
-

4.2 Policy Learning with Learned Dynamics

After we learn the target dynamics, we perform model-based offline RL training. During the policy optimization, we roll out new target data from the learned *target* dynamics with current policy and state in the offline data and keep the rollout data in the $\mathcal{D}_{\text{fake}}$. Also, we want to utilize the source data to optimize the policy. We follow the previous work DARA (Liu et al., 2022) on off-dynamics offline RL to first perform reward augmentation on the source data denoted as $\mathcal{D}_{\text{src.aug}}$. Our *enhanced target data* is $\mathcal{D}_{\text{src.aug}} \cup \mathcal{D}_{\text{trg}} \cup \mathcal{D}_{\text{fake}}$.

Reward modification with DARA In the off-dynamics offline RL setting, though we have learned the target domain transition, we still need to utilize the source domain data to optimize a policy for the target domain as the target domain data is limited and the learned dynamics might be inaccurate. Here, we follow the DARA (Liu et al., 2022) and DARC (Eysenbach et al., 2020) to utilize the reward shaping/augmentation method for the source transition to account for the dynamics mismatch, which is $r_{\text{aug}}(s, a, s') := r_{\text{src}}(s, a) + \eta \Delta r(s, a, s')$ and $\Delta r(s, a, s') = \log \frac{p_{\text{trg}}(s'|s, a)}{p_{\text{src}}(s'|s, a)}$. The Δr penalizes the transition if the transition is unlikely to appear in the target domain through a domain classifier and we refer the details to Appendix A.1. We denote the reward augmented source data as $\mathcal{D}_{\text{src.aug}}$.

Learning the Q function We learn the Q functions following standard temporal difference learning with *enhanced target data*:

$$\min \mathcal{L}_Q = \min \mathbb{E}_{\mathcal{D}_{\text{src.aug}} \cup \mathcal{D}_{\text{trg}} \cup \mathcal{D}_{\text{fake}}} \left[\left(r + \gamma \max_{a'} Q_{\theta^-}(s', a') - Q_{\theta}(s, a) \right)^2 \right]. \quad (4.8)$$

Policy optimization with Q weighted behavior cloning In offline RL, one key challenge is the exploration error as we are unable to properly evaluate out-of-distribution actions. This issue can be more severe in the off-dynamics offline setting. Behavior cloning (Fujimoto and Gu, 2021; Goecks et al., 2019) is a simple and efficient way to regularize the policy by pushing the policy to favor the actions in the offline dataset. However, in off-dynamics RL setting, when trained with both source

and target data, simply pushing the policy to favor actions in the offline dataset might harm the performance, especially actions from the source domain. Action in the source data might receive high *source* Q value/return in the source domain but might perform differently in the target domain due to the dynamics mismatch. So we cannot simply use the behavior cloning loss to regularize the policy. Instead, inspired by the advantage weighted regression (Kostrikov et al., 2021a), we can re-weight the behavior cloning loss with the *target* Q value, namely a Q weighted behavior cloning loss, where the Q value is learned with *enhanced target data*, so that this Q value approximate the Q value in the target domain. Then, the policy loss with Q weighted behavior cloning loss is:

$$\begin{aligned} \pi = \arg \min_{\pi} & -\mathbb{E}_{(s,a) \in D_{\text{src.aug}} \cup D_{\text{trg}} \cup D_{\text{fake}}} [\lambda Q(s, \pi(s))] \\ & + \mathbb{E}_{(s,a) \in D_{\text{src.aug}} \cup D_{\text{trg}}} \left[\exp \left(\frac{Q(s, \pi(s))}{1/N \sum_i^N |Q(s_i, \pi(s_i))|} \right) (\pi(s) - a)^2 \right], \end{aligned} \quad (4.9)$$

where the $\lambda = \frac{\alpha}{1/N \sum_i^N |Q(s_i, \pi(s_i))|}$ is the scaler λ that balance the behavior regularization error and Q loss and α is a hyper parameters.

The policy loss consists of two terms. One is maximizing the Q value given the *enhanced target data*. The other one is the Q-weighted behavior regularization loss, which pushes the policy to be close to actions that have high *target* Q value and also exists in the offline source and target dataset. We summarize the MOBODY in Algorithm 2.

Algorithm 2 MOBODY: Model-Based Off-dynamics Offline Reinforcement Learning

- 1: **Input:** Offline dataset $\mathcal{D}_{\text{src}} = \{(s, a, r, s')\}$ and $\mathcal{D}_{\text{trg}} = \{(s, a, r, s')\}$, $D_{\text{fake}} = \{\}$, number of model learning steps N_{model} , policy training steps N_{policy} .
 - 2: **Initialize:** Dynamics model, policy π_{θ} , rollout length L_{rollout} .
 - Dynamics Training**
 - 3: Learn target dynamics and reward estimation: $\hat{T}_{\text{trg}}, \hat{r}_{\text{trg}} \leftarrow$ Call Algorithm 1
 - Offline Policy Learning**
 - 4: Augment source data $\mathcal{D}_{\text{src.aug}} = \{(s, a, r + \eta \Delta r, s')\}$ with DARA.
 - 5: **for** $j = 1$ to N_{policy} **do**
 - 6: Collect rollout data from \hat{T} and \hat{r}_{trg} starting from state in $D_{\text{src.aug}}$ and D_{trg} . Add batch data to replay buffer D_{fake} .
 - 7: Sample batch $(s, a, s', r)_{\text{fake}}$ from $\mathcal{D}_{\text{fake}}$, $(s, a, s', r)_{\text{trg}}$ from \mathcal{D}_{trg} and $(s, a, s', r)_{\text{trg.aug}}$ from $\mathcal{D}_{\text{src.aug}}$. Concatenate them as $(s, a, s', r)_{\text{train}}$.
 - 8: Learn the Q value function with Equation (4.8)
 - 9: Update policy π_{θ} with Equation (4.9)
 - 10: **end for**
 - 11: **Return:** Learned policy π_{θ}
-

5 Experiments

In this section, we empirically evaluate MOBODY in off-dynamics offline RL settings using four MuJoCo environments from the ODRL benchmark: HalfCheetah-v2, Ant-v2, Walker2d-v2, and

Hopper-v2. We compare our method against several strong baselines and demonstrate its superior performance under various dynamics shifts. The code is available at [GitHub Repository](#).

5.1 Experimental Setup

Task and Environments. We evaluate MOBODY on the MuJoCo environments from the ODRL benchmark (Lyu et al., 2024b), which provides a standard testbed for evaluating off-dynamics offline RL method, including different environments, dynamics mismatch and shift levels. We set the original MuJoCo environment as the source domain. We focus on two types of dynamics shifts, gravity and friction, each scaled at four levels: $\{0.1, 0.5, 2.0, 5.0\}$ for the **target** domain by multiplying the original values in MuJoCo. These changes result in 32 settings ($4 \text{ tasks} \times 2 \text{ shift types} \times 4 \text{ levels}$). Each setting is denoted as **Environment-dynamics shift-shift level** for convenience, e.g., HalfCheetah-Gravity-0.1. We evaluate the performance with the **Normalized Score**, defined as: $normalized_score = \frac{score - random_score}{expert_score - random_score} \times 100$, where the *random_score* is achieved by the random policy and the *expert_score* is achieved by the SAC (Haarnoja et al., 2018) trained to the expert level in the target domain.

Dataset. We follow the ODRL benchmark and evaluate MOBODY using medium-level offline datasets. The target dataset is collected by the ODRL benchmark from mismatched environment, and the source dataset is collected by the D4RL benchmark (Fu et al., 2020). Both source and target datasets are collected independently using a SAC-trained behavior policy tuned to achieve about 50% of expert performance. The target data contains only 5,000 transitions, and the source data contains 1M transitions.

Baselines. We compare MOBODY with several baseline methods, including the model-free offline RL algorithms, model-based offline RL algorithms, and off-dynamics offline RL algorithms. For the model-free offline RL methods, we choose the IQL (Kostrikov et al., 2021a) and TD3-BC (Fujimoto and Gu, 2021) as they demonstrate good performance without any modification designed for solving off-dynamics offline RL problems. We directly train these baselines on the combined offline dataset with the source and target data. We select the MOPO (Yu et al., 2020) as the model-based offline RL baselines. Since directly training dynamics on the target domain has poor performance, we train the dynamics model of MOPO on the combined dataset and train the RL policy with the dynamics model and the combined dataset. We also incorporate the well-established off-dynamics offline RL methods, including DARA (Liu et al., 2022) and BOSA (Liu et al., 2024a).

5.2 Main Results

In [Table 1](#), we show the detailed results and highlight the best and second-best scores. In the last column, we report the percentage improvement or drop of our method compared to the best-performing baseline. Our proposed MOBODY outperforms baselines in 28 out of 32 settings, with competitive performance in the remaining four.

In detail, MOBODY significantly outperforms baselines in several hard settings, such as the HalfCheetah-Friction-0.1, Ant-Gravity-0.5, and Walker2d-Gravity-5.0, where other methods achieve extremely poor performance. In the last row of [Table 1](#), we sum the normalized scores in total. We find that DARA and BOSA do not have significant improvements compared with IQL and IQL achieves the best performance among the baselines in total score. Furthermore, our MOBODY

Table 1: Performance of MOBODY and baselines on MuJoCo tasks (HalfCheetah, Ant, Walker2D, Hopper) under medium-level offline dataset with dynamics shifts in gravity and friction at levels 0.1, 0.5, 2.0, 5.0. Source domains remain unchanged; target domains are shifted. We report normalized target-domain scores (mean \pm std over three seeds). Improvements are marked in \uparrow and degradations in \downarrow in the last column. Best and second-best scores are highlighted in **cyan** and **light cyan**, respectively.

Env	Level	BOSA	IQL	TD3-BC	MOPO	DARA	MOBODY	$\uparrow\downarrow$
HalfCheetah Gravity	0.1	9.31 \pm 1.94	9.62 \pm 4.27	6.90 \pm 0.34	6.28 \pm 0.22	12.90 \pm 1.01	14.18 \pm 1.06	9.92% \uparrow
	0.5	43.96 \pm 5.68	44.23 \pm 2.93	6.38 \pm 3.91	40.20 \pm 7.20	46.11 \pm 1.93	47.18 \pm 1.23	2.32% \uparrow
	2.0	27.86 \pm 0.94	31.34 \pm 1.68	29.29 \pm 3.62	21.89 \pm 10.49	31.85 \pm 1.31	41.60 \pm 7.35	30.61% \uparrow
	5.0	17.95 \pm 11.97	44.00 \pm 23.13	73.75 \pm 14.11	57.75 \pm 18.92	27.67 \pm 17.01	83.05 \pm 1.21	12.61% \uparrow
HalfCheetah Friction	0.1	12.53 \pm 3.61	26.39 \pm 11.35	8.95 \pm 0.71	28.32 \pm 9.23	23.69 \pm 16.46	57.53 \pm 2.49	103.14% \uparrow
	0.5	68.93 \pm 0.35	69.80 \pm 0.64	49.43 \pm 9.91	54.98 \pm 5.91	64.89 \pm 3.04	69.54 \pm 0.48	0.37% \downarrow
	2.0	46.53 \pm 0.37	46.04 \pm 2.04	43.51 \pm 0.74	42.33 \pm 3.89	46.25 \pm 2.36	50.02 \pm 3.26	45.00% \uparrow
	5.0	44.07 \pm 9.07	44.96 \pm 6.78	35.83 \pm 6.65	42.39 \pm 10.22	40.06 \pm 7.87	59.20 \pm 4.91	31.67% \uparrow
Ant Gravity	0.1	25.58 \pm 2.21	12.53 \pm 1.11	13.23 \pm 2.61	8.93 \pm 1.23	11.03 \pm 1.24	37.09 \pm 2.12	45.00% \uparrow
	0.5	19.03 \pm 4.41	10.09 \pm 2.00	12.91 \pm 2.85	12.28 \pm 3.88	9.04 \pm 1.35	37.44 \pm 2.79	96.74% \uparrow
	2.0	41.77 \pm 1.52	37.17 \pm 0.96	34.04 \pm 4.12	35.43 \pm 3.22	36.64 \pm 0.82	45.83 \pm 1.71	9.72% \uparrow
	5.0	31.94 \pm 0.69	31.59 \pm 0.35	6.37 \pm 0.45	28.97 \pm 5.93	31.01 \pm 0.39	65.45 \pm 3.23	104.92% \uparrow
Ant Friction	0.1	58.95 \pm 0.71	55.56 \pm 0.46	49.20 \pm 2.55	49.86 \pm 5.99	55.12 \pm 0.24	58.79 \pm 0.11	0.27% \downarrow
	0.5	59.72 \pm 3.57	59.28 \pm 0.80	25.21 \pm 7.17	32.28 \pm 3.25	58.92 \pm 0.80	62.41 \pm 4.10	4.50% \uparrow
	2.0	20.18 \pm 3.79	19.84 \pm 3.20	22.69 \pm 8.10	15.93 \pm 0.87	17.54 \pm 2.47	47.41 \pm 4.40	108.95% \uparrow
	5.0	9.07 \pm 0.88	7.75 \pm 0.25	10.06 \pm 4.16	13.89 \pm 3.2	7.80 \pm 0.12	31.17 \pm 5.57	124.41% \uparrow
Walker2d Gravity	0.1	18.75 \pm 12.02	16.04 \pm 7.60	36.48 \pm 0.95	41.98 \pm 10.13	20.12 \pm 5.74	65.85 \pm 5.08	56.86% \uparrow
	0.5	40.09 \pm 20.37	42.05 \pm 10.52	27.43 \pm 3.92	40.32 \pm 8.78	29.72 \pm 16.02	43.57 \pm 2.32	3.61% \uparrow
	2.0	8.91 \pm 2.28	25.69 \pm 10.70	11.88 \pm 9.38	28.79 \pm 3.07	32.20 \pm 1.05	44.32 \pm 4.58	37.64% \uparrow
	5.0	5.25 \pm 0.50	5.42 \pm 0.29	5.12 \pm 0.18	5.65 \pm 0.99	5.44 \pm 0.08	46.05 \pm 20.73	715.04% \uparrow
Walker2d Friction	0.1	7.88 \pm 1.88	5.72 \pm 0.23	29.60 \pm 24.90	27.99 \pm 2.11	5.65 \pm 0.06	28.23 \pm 9.13	4.63% \downarrow
	0.5	63.94 \pm 20.40	66.26 \pm 3.03	45.01 \pm 18.98	60.81 \pm 3.04	68.81 \pm 1.12	76.96 \pm 1.99	11.84% \uparrow
	2.0	39.06 \pm 17.36	65.40 \pm 7.13	67.89 \pm 1.66	68.38 \pm 1.09	72.91 \pm 0.37	73.74 \pm 0.49	1.14% \uparrow
	5.0	10.07 \pm 4.91	5.39 \pm 0.03	5.76 \pm 0.84	5.34 \pm 1.61	5.36 \pm 0.28	27.38 \pm 3.87	171.90% \uparrow
Hopper Gravity	0.1	27.82 \pm 13.41	13.10 \pm 0.98	15.59 \pm 6.09	22.49 \pm 3.71	23.40 \pm 11.62	36.25 \pm 1.50	30.30% \uparrow
	0.5	28.54 \pm 12.77	16.24 \pm 7.89	23.00 \pm 14.87	23.92 \pm 1.91	12.86 \pm 0.18	33.57 \pm 6.71	17.62% \uparrow
	2.0	11.84 \pm 2.37	16.10 \pm 1.64	18.62 \pm 6.88	11.76 \pm 0.32	14.65 \pm 2.47	23.79 \pm 2.09	27.77% \uparrow
	5.0	7.36 \pm 0.13	8.12 \pm 0.16	9.08 \pm 1.15	7.77 \pm 0.31	7.90 \pm 1.27	8.06 \pm 0.03	11.23% \downarrow
Hopper Friction	0.1	25.55 \pm 2.69	24.16 \pm 4.50	18.64 \pm 3.37	34.32 \pm 6.79	26.13 \pm 4.24	51.19 \pm 2.56	49.16% \uparrow
	0.5	25.22 \pm 4.48	23.56 \pm 1.68	19.60 \pm 15.45	12.32 \pm 3.96	26.94 \pm 2.86	41.34 \pm 0.49	53.45% \uparrow
	2.0	10.32 \pm 0.06	10.15 \pm 0.06	9.89 \pm 0.20	10.99 \pm 0.76	10.15 \pm 0.03	11.00 \pm 0.14	0.09% \uparrow
	5.0	7.90 \pm 0.06	7.93 \pm 0.01	7.80 \pm 1.04	7.68 \pm 0.19	7.86 \pm 0.05	8.07 \pm 0.04	1.77% \uparrow
Total		875.88	901.52	779.14	893.22	890.62	1427.26	58.35% \uparrow

achieve 58.35% improvements compared with the best baseline methods, which is significantly better than the baselines. These empirical results underscore the superior performance of MOBODY in solving the off-dynamics offline RL problem and the potential in real-world applications where dynamics shifts are prevalent.

Figure 3 summarizes the normalized scores across all environments under different shift levels. In Figure 3a, MOBODY consistently outperforms baselines under gravity shifts, with especially large gains at the more challenging and larger shift levels on 0.1 and 5.0 as the MOBODY can explore more on the environment with the learned dynamics. A similar trend is observed in Figure 3b, where MOBODY again outperforms all baselines, with greater improvements in the larger shift (0.1

and 5.0) compared to the smaller ones (0.5 and 2.0).

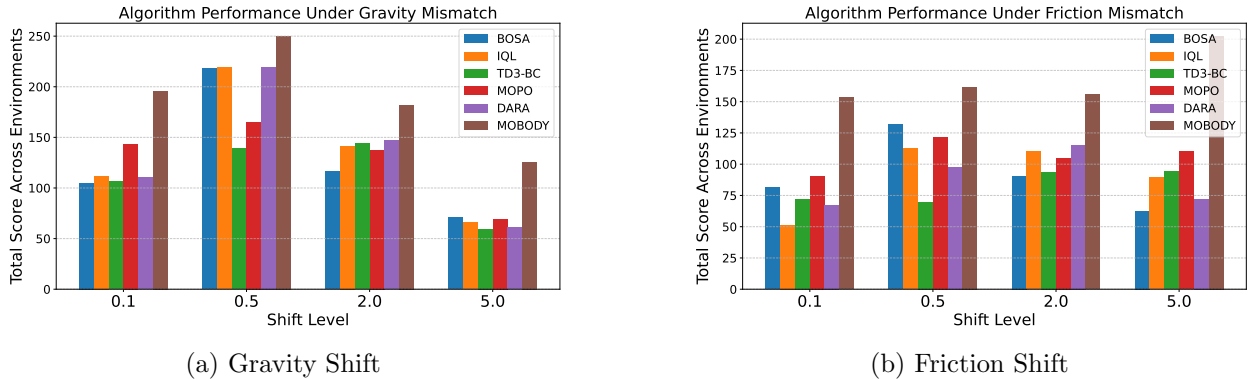


Figure 3: Performance of our MOBODY and baselines in different dynamics shift with various shift levels $\{0.1, 0.5, 2.0, 5.0\}$. The scores are summed over all the environments (HalfCheetah, Ant, Walker2D, and Hopper) in the target domain. We directly compare the algorithms in the same dynamics shift levels. The higher scores indicate better performance. We can observe a larger improvement for larger shift cases (0.1 and 5.0).

5.3 Ablation Study

In this section, we conduct ablation studies on two main components of MOBODY: dynamics learning and policy learning. We first evaluate the overall effectiveness of each component, then analyze specific design choices. For dynamics learning, we assess the impact of the cycle transition loss and representation learning. For policy learning, we examine the effectiveness of the Q-weighted loss. We evaluate on the Walker2d environments as discussed in Section 5.1. The ablation study results are shown in Table 2.

We first evaluate the performance of our proposed dynamics learning and policy learning by replacing the dynamics learning with the existing dynamics learning model or the policy learning with the existing offline RL algorithm. We denote the two ablation studies as follows:

A1: Replace dynamics learning We compare our MOBODY with a variant replacing the dynamics learning with the existing model-based method. We use a black-box dynamics model trained on **target data only**, while the policy learning follows the same method as in MOBODY. Table 2 demonstrates that the **A1** variant is significantly degraded compared with our proposed MOBODY algorithm in Walker2d. This indicates that only using the existing dynamics models trained on the target data is insufficient to rollout trajectories in the target domain. This motivates us to propose a novel dynamics model learning method.

A2: Replace policy learning Similar to the **A1**, we replace the policy learning with the existing offline RL algorithm. We adopt the same dynamics learning approach as in MOBODY and use Conservative Q-Learning (CQL) (Kumar et al., 2020) for policy learning. Table 2 shows that our proposed MOBODY outperforms the **A2** variant in Walker2d. This demonstrates that the policy learning part of our proposed MOBODY with Q-weight behavior cloning can better utilize

Table 2: Performance of ablation study of our proposed MOBODY method. A1-A4 represent four different ablation studies detailed in Section 5.3. The experiments are conducted on the Walker2d environments under the medium-level with dynamics shifts in gravity and friction in $\{0.1, 0.5, 2.0, 5.0\}$ shift levels. The source domains are the original environments and the target domains are the environments with dynamics shifts. We report the normalized scores in the target domain with the mean and standard deviation across three random seeds. The higher scores indicate better performance.

Env	Level	Algorithm Ablation		Loss Ablation		MOBODY
		A1	A2	A3	A4	
Walker2d Gravity	0.1	55.23 ± 10.22	55.43 ± 5.31	35.34 ± 10.97	19.53 ± 4.68	65.85 ± 5.08
	0.5	35.66 ± 3.11	39.98 ± 1.32	30.63 ± 2.92	24.44 ± 1.91	43.57 ± 2.32
	2.0	31.94 ± 5.32	28.58 ± 5.59	34.42 ± 3.60	47.13 ± 2.44	44.32 ± 4.58
	5.0	3.56 ± 0.79	11.37 ± 3.91	4.42 ± 1.20	6.43 ± 0.32	46.05 ± 20.73
Walker2d Friction	0.1	24.34 ± 10.33	25.73 ± 2.43	21.42 ± 3.85	19.48 ± 4.32	28.23 ± 9.13
	0.5	56.31 ± 7.17	73.23 ± 3.73	68.53 ± 4.14	61.38 ± 6.84	76.96 ± 1.99
	2.0	60.52 ± 5.82	71.14 ± 2.59	67.98 ± 6.96	76.44 ± 6.43	73.74 ± 0.49
	5.0	4.32 ± 0.85	18.32 ± 2.18	5.42 ± 0.82	7.89 ± 1.33	27.38 ± 3.87
Hopper Gravity	0.1	14.53 ± 2.81	28.07 ± 4.12	33.65 ± 3.21	11.54 ± 1.12	36.25 ± 1.50
	0.5	28.83 ± 3.32	25.70 ± 1.86	23.52 ± 3.33	20.11 ± 1.26	33.57 ± 6.71
	2.0	10.64 ± 1.92	12.32 ± 5.21	10.90 ± 1.29	16.40 ± 4.12	23.79 ± 2.09
	5.0	8.12 ± 0.69	8.23 ± 1.92	8.79 ± 0.94	8.89 ± 1.01	8.06 ± 0.03
Hopper Friction	0.1	26.09 ± 4.75	35.14 ± 7.97	24.42 ± 2.86	20.07 ± 10.32	51.19 ± 2.56
	0.5	22.42 ± 3.32	31.31 ± 5.08	29.26 ± 6.02	27.07 ± 3.73	41.34 ± 0.49
	2.0	10.64 ± 0.32	9.41 ± 1.03	10.31 ± 0.12	8.47 ± 1.13	11.00 ± 0.14
	5.0	8.43 ± 1.32	7.52 ± 0.29	8.14 ± 0.91	7.55 ± 1.02	8.07 ± 0.04

the dynamics model compared with the existing method.

Then we delve into the details of the dynamics learning and policy learning part especially our designs of the loss function and Q-weighting. We have the following ablation studies:

A3: No Cycle Transition Loss Here, the dynamics model follows the dynamics learning of the proposed MOBODY, but without the cycle transition loss. We hope to evaluate the effectiveness of our proposed cycle transition loss. Table 2 illustrates the **A3** suffers degradations compared with our MOBODY in most of the settings. This indicates that the cycle transition loss helps learn a better state representation in our proposed MOBODY method.

A4: No Q-weighted Similar to the **A3**, we compare our MOBODY with the a variant without the Q-weighted behavior cloning loss. We keep the same dynamics learning method as our proposed MOBODY and replace the Q-weighted behavior cloning loss with the vanilla behavior cloning loss. In Table 2, our method outperforms the method without the Q-weighted behavior cloning in Walker2d. The **A4** underperforms MOBODY in most of the settings except the Walker2d 2.0 level where all settings have similar performance. This suggests that our proposed Q-weighted approach can help regularize the policy learning in the off-dynamics offline RL scenarios.

6 Conclusion

In this work, we study the off-dynamics offline reinforcement learning problem through a model-based offline RL method. We introduce MOBODY, a model-based offline RL algorithm that enables policy exploration in the target domain via learned dynamics models. By leveraging shared latent representations across domains, MOBODY effectively learns target dynamics using both source and limited target data. Additionally, we propose a Q-weighted behavior cloning strategy that favors actions with high target Q value, further improving policy learning. Experimental results on MuJoCo benchmarks demonstrate that MOBODY consistently outperforms prior methods, particularly in scenarios with significant dynamics mismatch, highlighting its robustness and generalization capability. Our method shows the potential of data augmentation in policy learning with a learned dynamics model. Future work includes further investigation on improving the dynamics learning.

A Experimental Details

A.1 The DARA Augmentation for Source Data Used in MOBODY

Note that in MOBODY, we use DARA to augment the reward in the source data. In this section, we introduce its technical details. Specifically, DARA (Liu et al., 2022) is an offline version of DARC (Eysenbach et al., 2020), where the key idea is to train domain classifiers to calculate the reward penalty term $\Delta r(s, a, s')$ that can be used to augment the rewards in the source domain dataset via

$$\hat{r}_{\text{DARA}}(s, a, s') = r(s, a, s') - \eta \Delta r(s, a, s'),$$

where η is the penalty coefficient which we set to 0.1 following the ODRL benchmark (Lyu et al., 2024b).

Estimation of the Δr . Following the DARC and DARA (Eysenbach et al., 2020; Liu et al., 2022), the reward augmentation Δr can be estimated with the following two binary classifiers $p(\text{trg}|s, a)$ and $p(\text{trg}|s, a, s')$ with Bayes' rules:

$$p(\text{trg}|s, a, s') = p_{\text{trg}}(s'|s, a)p(s, a|\text{trg})p(\text{trg})/p(s, a, s'), \quad (\text{A.1})$$

and

$$p(s, a|\text{trg}) = p(\text{trg}|s, a)p(s, a)/p(\text{trg}). \quad (\text{A.2})$$

Replacing the $p(s, a|\text{trg})$ in Eq. (A.1) with Eq. (A.2), we obtain

$$p_{\text{trg}}(s'|s, a) = \frac{p(\text{trg}|s, a, s')p(s, a, s')}{p(\text{trg}|s, a)p(s, a)}.$$

Similarly, we can obtain the $p_{\text{src}}(s'|s, a) = \frac{p(\text{src}|s, a, s')p(s, a, s')}{p(\text{src}|s, a)p(s, a)}$. Then we can calculate $\Delta r(s, a, s')$ as

follows:

$$\begin{aligned}\Delta r(s, a, s') &= \log \left(\frac{p_{\text{trg}}(s'|s, a)}{p_{\text{src}}(s'|s, a)} \right) \\ &= \log p(\text{trg}|s, a, s') - \log p(\text{trg}|s, a) + \log p(\text{src}|s, a, s') - \log p(\text{src}|s, a).\end{aligned}$$

Training the Classifier $p(\text{trg}|s, a)$ and $p(\text{trg}|s, a, s')$. The two classifiers are parameterized by θ_{SA} and θ_{SAS} . To update the two classifiers, we sample one mini-batch of data from the source replay buffer D_{src} and the target replay buffer D_{trg} respectively. To address data imbalance, we sample an equal number of data points from both the source and target domain buffers in each mini-batch. Then, the parameters are learned by minimizing the standard cross-entropy loss:

$$\begin{aligned}\mathcal{L}_{\text{SAS}} &= -\mathbb{E}_{D_{\text{src}}} [\log p_{\theta_{\text{SAS}}}(\text{src}|s, a, s')] - \mathbb{E}_{D_{\text{trg}}} [\log p_{\theta_{\text{SAS}}}(\text{trg}|s, a, s')] , \\ \mathcal{L}_{\text{SA}} &= -\mathbb{E}_{D_{\text{src}}} [\log p_{\theta_{\text{SA}}}(\text{src}|s, a)] - \mathbb{E}_{D_{\text{trg}}} [\log p_{\theta_{\text{SA}}}(\text{trg}|s, a)] .\end{aligned}$$

Thus, $\theta = (\theta_{\text{SAS}}, \theta_{\text{SA}})$ is obtained from the following optimization problem

$$\theta = \underset{\theta}{\operatorname{argmin}} \mathcal{L}_{CE}(D_{\text{src}}, D_{\text{trg}}) = \underset{\theta}{\operatorname{argmin}} [\mathcal{L}_{\text{SAS}} + \mathcal{L}_{\text{SA}}].$$

A.2 Technical Details about Baseline Algorithms

In this section, we introduce the baselines in detail and the implementation follows the ODRL benchmark (Lyu et al., 2024b).

BOSA (Liu et al., 2024a). BOSA deals with the out-of-distribution (OOD) state actions pair through a supported *policy* optimization and addresses the OOD dynamics issue through a supported *value* optimization by data filtering. Specifically, the policy is updated by maximizing the following objective function:

$$\mathcal{L}_{\text{actor}} = \mathbb{E}_{s \sim D_{\text{src}} \cup D_{\text{trg}}, a \sim \pi_{\phi}(s)} [Q(s, a)], \quad \text{s.t.} \quad \mathbb{E}_{s \sim D_{\text{src}} \cup D_{\text{trg}}} [\hat{\pi}_{\theta_{\text{offline}}}(\pi_{\theta}(s)|s)] > \epsilon.$$

Here, the ϵ is the threshold, $\hat{\pi}_{\theta_{\text{offline}}}$ is the learned policy for the combined offline dataset. The value function is updated with

$$\begin{aligned}\mathcal{L}_{\text{critic}} &= \mathbb{E}_{(s,a) \sim D_{\text{src}}} [Q(s, a)] \\ &\quad + \mathbb{E}_{(s,a,r,s') \sim D_{\text{src}} \cup D_{\text{trg}}, a' \sim \pi_{\phi}(\cdot|s)} [I(\hat{p}_{\text{trg}}(s'|s, a) > \epsilon') (Q_{\theta_i}(s, a) - y)^2],\end{aligned}$$

where $I(\cdot)$ is the indicator function, $\hat{p}_{\text{trg}}(s'|s, a) = \operatorname{argmax}_{s'} E_{(s,a,s') \sim D_{\text{trg}}} [\log \hat{p}_{\text{trg}}(s'|s, a)]$ is the estimated target domain dynamics and ϵ' is the threshold.

IQL (Kostrikov et al., 2021a). IQL learns the state value function and state-action value function simultaneously by minimizing the following expectile regression loss function

$$\mathcal{L}_V = \mathbb{E}_{(s,a) \sim D_{\text{src}} \cup D_{\text{trg}}} [L_2^{\tau}(Q_{\theta}(s, a) - V_{\psi}(s))],$$

where $L_2^{\tau}(u) = |\tau - I(u < 0)| |u|^2$, $I(\cdot)$ is the indicator function, and θ is the target network parameter.

The state-action value function is then updated by

$$\mathcal{L}_Q = \mathbb{E}_{(s,a,r,s') \sim \mathcal{D}_{\text{src}} \cup \mathcal{D}_{\text{trg}}} \left[\left(r(s,a) + \gamma V_\psi(s') - Q_\theta(s,a) \right)^2 \right].$$

The advantage function is $A(s,a) = Q(s,a) - V(s)$. The policy is optimized by the advantage-weighted behavior cloning

$$\mathcal{L}_{\text{actor}} = \mathbb{E}_{(s,a) \sim \mathcal{D}_{\text{src}} \cup \mathcal{D}_{\text{trg}}} [\exp(\beta \cdot A(s,a)) \log \pi_\phi(a|s)],$$

where β is the inverse temperature coefficient.

TD3-BC (Fujimoto and Gu, 2021). TD3-BC is an effective model-free offline RL approach that incorporates a behavior cloning regularization term into the objective function of the vanilla TD3. The policy optimization loss is

$$\mathcal{L}_{\text{actor}} = \lambda \cdot \mathbb{E}_{s \sim \mathcal{D}_{\text{src}} \cup \mathcal{D}_{\text{trg}}} [Q(s, \pi_\theta(s))] + \mathbb{E}_{(s,a) \sim \mathcal{D}_{\text{src}} \cup \mathcal{D}_{\text{trg}}} [(a - \pi_\theta(s))^2],$$

where $\lambda = \frac{\nu}{\frac{1}{N} \sum_{(s_j, a_j)} Q(s_j, a_j)}$ and $\nu \in \mathbb{R}^+$ is the normalization coefficient.

MOPO (Yu et al., 2020). MOPO is a standard model-based offline policy optimization method that first learns a dynamics model and then penalizes rewards based on model uncertainty. The policy is subsequently optimized using SAC (Haarnoja et al., 2018). Following prior off-dynamics work in the online setting (Eysenbach et al., 2020), which uses MBPO as a baseline, we train the dynamics model using a combination of offline source and target domain data. Our implementation follows the OfflineRL-Kit framework.

DARA (Liu et al., 2022). We refer to [Appendix A.1](#) for the details. We follow the implementation in ODRL (Lyu et al., 2024b).

A.3 Experiment Details

In this section, we present the hyperparameters used for our method and the baselines. Detailed configurations are provided in [Table 3](#). We follow the setup from the ODRL benchmark (Lyu et al., 2024b). To ensure a fair comparison, we use a transition network with architecture (256, 256, 256) for MOPO, instead of the original (256, 256), to match the increased capacity of our dynamics model.

Hyperparameter Tuning. We tune the hyperparameters for rollout length and the behavior cloning (BC) regularization weight, as summarized in [Table 3](#). Specifically, the weight λ in [Equation \(4.9\)](#), which is the weight of the Q-weighted behavior cloning loss, is chosen from the set 0.1, 1, 10. Also, the rollout length using the learned dynamics model is tuned over 1, 2, 3. For TD3-BC, which also has a BC regularization, we similarly tune the BC weight in 0.1, 1, 10. For MOPO, we tune the rollout length over the same range 1, 2, 3. As for weight in [Equation \(4.7\)](#), which controls the weight of the cycle-consistency transition loss and encoder loss, we fix it to 1 across all tasks, as varying λ did not lead to significant performance differences in our experiments.

For each set of hyperparameters, we run experiments with three different random seeds and select the best-performing configuration based on the average performance across these runs. Final results are reported at 1 million training steps.

Computational Resources. All experiments are conducted on a single GPU (NVIDIA RTX A5000, 24,564 MiB) with 8 CPUs (AMD Ryzen Threadripper 3960X, 24-core). Each run requires approximately 12 GB of RAM and 20 GB of available disk space for data storage.

Table 3: Hyperparameters of MOBODY and baselines.

Hyperparameter	Value
Shared	
Actor network	(256, 256)
Critic network	(256, 256)
Learning rate	3×10^{-4}
Optimizer	Adam
Discount factor	0.99
Replay buffer size	10^6
Nonlinearity	ReLU
Target update rate	5×10^{-3}
Source domain Batch size	128
Target domain Batch size	128
MOBODY	
Latent dimensions	16
State encoder	(256, 256)
State action encoder	(32)
Transition	(256, 256)
Representation penalty λ	1
Rollout length	1, 2 or 3
Reward Penalty	5
Q-weighted behavior cloning	0.1, 1 or 10
Classifier Network	(256, 256)
Reward penalty coefficient λ	0.1
DARA	
Temperature coefficient	0.2
Maximum log std	2
Minimum log std	-20
Classifier Network	(256, 256)
Reward penalty coefficient λ	0.1
BOSA	
Temperature coefficient	0.2
Maximum log std	2
Minimum log std	-20
Policy regularization coefficient λ_{policy}	0.1
Transition coefficient $\lambda_{\text{transition}}$	0.1
Threshold parameter ϵ, ϵ'	$\log(0.01)$

Hyperparameter	Value
Value weight ω	0.1
CVAE ensemble size	1 for the behavior policy, 5 for the dynamics model
IQL	
Temperature coefficient	0.2
Maximum log std	2
Minimum log std	-20
Inverse temperature parameter β	3.0
Expectile parameter τ	0.7
TD3-BC	
Normalization coefficient ν	2.5
BC regularization loss	0.1, 1 or 10
MOPO	
Transition	(256, 256, 256)
Maximum log std	2
Minimum log std	-20
Reward penalty τ	5.0
Rollout Length	1, 2 or 3

A.4 Environment Setting

Gravity Shift. Following the ODRL benchmark (Lyu et al., 2024b), we modify the gravity of the environment by editing the gravity attribute. For example, the gravity of the HalfCheetah in the target is modified to 0.5 times the gravity in the source domain with the following code.

```
# gravity
<option gravity="0 0 -4.905" timestep="0.01"/>
```

Friction Shift. The friction shift is generated by modifying the friction attribute in the geom elements. The frictional components are adjusted to $\{0.1, 0.5, 2.0, 5.0\}$ times the frictional components in the source domain, respectively.

B Limitation

MOBODY relies on the assumption that the source and target domains share a common state representation ϕ_E and transition ϕ_T . In future work, we plan to explore how to effectively learn a dynamics model for the target domain when this assumption does not hold.

C Impact Statement

MOBODY avoids training a policy in a high-risk environment and only requires very limited offline high-risk environments to train a policy. This significantly reduces the risks in safety-critical tasks where collecting data and exploration in the target domain is hard. Potentially, in the future, we can extend our work to high-risk environments, such as autonomous driving and real-world robot manipulation, where there are real safety constraints that need to be satisfied.

References

- BARRETO, A., DABNEY, W., MUNOS, R., HUNT, J., SCHAUL, T., SILVER, D. and VAN HASSELT, H. (2017). Successor features for transfer in reinforcement learning. In *Advances in Neural Information Processing Systems*, vol. 30. 4
- BOTTEGHI, N., POEL, M. and BRUNE, C. (2025). Unsupervised representation learning in deep reinforcement learning: A review. *IEEE Control Systems* 45 26–68. 4
- EYSENBACH, B., ASAWA, S., CHAUDHARI, S., LEVINE, S. and SALAKHUTDINOV, R. (2020). Off-dynamics reinforcement learning: Training for transfer with domain classifiers. *arXiv preprint arXiv:2006.13916* . 3, 4, 8, 14, 16
- FU, J., KUMAR, A., NACHUM, O., TUCKER, G. and LEVINE, S. (2020). D4rl: Datasets for deep data-driven reinforcement learning. *arXiv preprint arXiv:2004.07219* . 10
- FUJIMOTO, S., CHANG, W.-D., SMITH, E. J., GU, S. S., PRECUP, D. and MEGER, D. (2023). For sale: State-action representation learning for deep reinforcement learning. In *Advances in Neural Information Processing Systems*. 4, 6
- FUJIMOTO, S. and GU, S. S. (2021). A minimalist approach to offline reinforcement learning. *Advances in neural information processing systems* 34 20132–20145. 3, 8, 10, 16
- FUJIMOTO, S., MEGER, D. and PRECUP, D. (2021). A deep reinforcement learning approach to marginalized importance sampling with the successor representation. In *International Conference on Machine Learning*. PMLR. 4
- GOECKS, V. G., GREMILLION, G. M., LAWHERN, V. J., VALASEK, J. and WAYTOWICH, N. R. (2019). Integrating behavior cloning and reinforcement learning for improved performance in dense and sparse reward environments. *arXiv preprint arXiv:1910.04281* . 8
- GUO, Y., WANG, Y., SHI, Y., XU, P. and LIU, A. (2024). Off-dynamics reinforcement learning via domain adaptation and reward augmented imitation. In *Advances in Neural Information Processing Systems*, vol. 37. 3, 4
- HAARNOJA, T., ZHOU, A., ABBEEL, P. and LEVINE, S. (2018). Soft actor-critic: Off-policy maximum entropy deep reinforcement learning with a stochastic actor. In *International conference on machine learning*. PMLR. 10, 16

- HANSEN, N., WANG, X. and SU, H. (2022a). Temporal difference learning for model predictive control. In *International Conference on Machine Learning (ICML)*. PMLR. 4
- HANSEN, N., WANG, X. and SU, H. (2022b). Temporal difference learning for model predictive control. *arXiv preprint arXiv:2203.04955* . 4, 6
- IYENGAR, G. N. (2005). Robust dynamic programming. *Mathematics of Operations Research* **30** 257–280. 3
- JIN, C., YANG, Z., WANG, Z. and JORDAN, M. I. (2020). Provably efficient reinforcement learning with linear function approximation. In *Conference on learning theory*. PMLR. 6
- KAEHLING, L. P., LITTMAN, M. L. and MOORE, A. W. (1996). Reinforcement learning: A survey. *Journal of artificial intelligence research* **4** 237–285. 1
- KARL, M., SOELCH, M., BAYER, J. and VAN DER SMAGT, P. (2017). Deep variational bayes filters: Unsupervised learning of state space models from raw data. In *International Conference on Learning Representations (ICLR)*. 4
- KIDAMBI, R., RAJESWARAN, A., NETRAPALLI, P. and JOACHIMS, T. (2020). Morel: Model-based offline reinforcement learning. *Advances in neural information processing systems* **33** 21810–21823. 4
- KINGMA, D. P., WELLING, M. ET AL. (2013). Auto-encoding variational bayes. 6, 7
- KIRAN, B. R., SOBH, I., TALPAERT, V., MANNION, P., AL SALLAB, A. A., YOGAMANI, S. and PÉREZ, P. (2021). Deep reinforcement learning for autonomous driving: A survey. *IEEE transactions on intelligent transportation systems* **23** 4909–4926. 1
- KOSTRIKOV, I., NAIR, A. and LEVINE, S. (2021a). Offline reinforcement learning with implicit q-learning. *arXiv preprint arXiv:2110.06169* . 3, 9, 10, 15
- KOSTRIKOV, I., YARATS, D. and FERGUS, R. (2021b). Image augmentation is all you need: Regularizing deep reinforcement learning from pixels. In *International Conference on Learning Representations (ICLR)*. 4
- KUMAR, A., ZHOU, A., TUCKER, G. and LEVINE, S. (2020). Conservative q-learning for offline reinforcement learning. *Advances in neural information processing systems* **33** 1179–1191. 12
- LEE, H., YOON, H.-K., KIM, J., PARK, J. S., KOO, C.-H., WON, D. and LEE, H.-C. (2023). Development and validation of a reinforcement learning model for ventilation control during emergence from general anesthesia. *npj Digital Medicine* **6** 145. 1
- LEVINE, S., KUMAR, A., TUCKER, G. and FU, J. (2020). Offline reinforcement learning: Tutorial, review, and perspectives on open problems. *arXiv preprint arXiv:2005.01643* . 2
- LI, Y. (2017). Deep reinforcement learning: An overview. *arXiv preprint arXiv:1701.07274* . 1

- LIU, G., ZHANG, C., ZHAO, L., QIN, T., ZHU, J., LI, J., YU, N. and LIU, T.-Y. (2021). Return-based contrastive representation learning for reinforcement learning. In *International Conference on Learning Representations (ICLR)*. 4
- LIU, J., ZHANG, H. and WANG, D. (2022). Dara: Dynamics-aware reward augmentation in offline reinforcement learning. *arXiv preprint arXiv:2203.06662* . 2, 3, 4, 8, 10, 14, 16
- LIU, J., ZHANG, Z., WEI, Z., ZHUANG, Z., KANG, Y., GAI, S. and WANG, D. (2024a). Beyond good state actions: Supported cross-domain offline reinforcement learning. In *Proceedings of the AAAI Conference on Artificial Intelligence*, vol. 38. 2, 3, 10, 15
- LIU, Z., WANG, W. and XU, P. (2024b). Upper and lower bounds for distributionally robust off-dynamics reinforcement learning. *arXiv preprint arXiv:2409.20521* . 3
- LIU, Z. and XU, P. (2024a). Distributionally robust off-dynamics reinforcement learning: Provable efficiency with linear function approximation. In *International Conference on Artificial Intelligence and Statistics*. PMLR. 3
- LIU, Z. and XU, P. (2024b). Minimax optimal and computationally efficient algorithms for distributionally robust offline reinforcement learning. In *The Thirty-eighth Annual Conference on Neural Information Processing Systems*. 3
- LU, M., ZHONG, H., ZHANG, T. and BLANCHET, J. (2024). Distributionally robust reinforcement learning with interactive data collection: Fundamental hardness and near-optimal algorithms. In *The Thirty-eighth Annual Conference on Neural Information Processing Systems*. 3
- LYU, J., BAI, C., YANG, J., LU, Z. and LI, X. (2024a). Cross-domain policy adaptation by capturing representation mismatch. *arXiv preprint arXiv:2405.15369* . 2, 3, 4
- LYU, J., XU, K., XU, J., YANG, J.-W., ZHANG, Z., BAI, C., LU, Z., LI, X. ET AL. (2024b). Odr: A benchmark for off-dynamics reinforcement learning. *Advances in Neural Information Processing Systems* **37** 59859–59911. 2, 4, 10, 14, 15, 16, 18
- NILIM, A. and EL GHAOU, L. (2005). Robust control of markov decision processes with uncertain transition matrices. *Operations Research* **53** 780–798. 3
- OTA, K., OIKI, T., JHA, D. K., MARIYAMA, T. and NIKOVSKI, D. (2020). Can increasing input dimensionality improve deep reinforcement learning? In *Proceedings of the 37th International Conference on Machine Learning*. PMLR. 4
- PARKER, W. S. (2013). Ensemble modeling, uncertainty and robust predictions. *Wiley interdisciplinary reviews: Climate change* **4** 213–223. 7
- PETERS, J. and SCHAAL, S. (2007). Reinforcement learning by reward-weighted regression for operational space control. In *Proceedings of the 24th international conference on Machine learning*. 3
- RASHIDINEJAD, P., ZHU, B., MA, C., JIAO, J. and RUSSELL, S. (2021). Bridging offline reinforcement learning and imitation learning: A tale of pessimism. *Advances in Neural Information Processing Systems* **34** 11702–11716. 4

- RIGTER, M., LACERDA, B. and HAWES, N. (2022). Rambo-rl: Robust adversarial model-based offline reinforcement learning. *Advances in neural information processing systems* **35** 16082–16097. [2](#), [4](#)
- SATIA, J. K. and LAVE JR, R. E. (1973). Markovian decision processes with uncertain transition probabilities. *Operations Research* **21** 728–740. [3](#)
- SHI, L. and CHI, Y. (2024). Distributionally robust model-based offline reinforcement learning with near-optimal sample complexity. *Journal of Machine Learning Research* **25** 1–91. [3](#)
- TANG, C., LIU, Z. and XU, P. (2024). Robust offline reinforcement learning with linearly structured f -divergence regularization. *arXiv preprint arXiv:2411.18612* . [3](#)
- WANG, R., YANG, Y., LIU, Z., ZHOU, D. and XU, P. (2024). Return augmented decision transformer for off-dynamics reinforcement learning . [2](#), [3](#)
- WEN, X., BAI, C., XU, K., YU, X., ZHANG, Y., LI, X. and WANG, Z. (2024). Contrastive representation for data filtering in cross-domain offline reinforcement learning. *arXiv preprint arXiv:2405.06192* . [2](#), [3](#), [4](#)
- WIESEMANN, W., KUHN, D. and RUSTEM, B. (2013). Robust markov decision processes. *Mathematics of Operations Research* **38** 153–183. [3](#)
- XU, H. and MANNOR, S. (2006). The robustness-performance tradeoff in markov decision processes. *Advances in Neural Information Processing Systems* **19**. [3](#)
- XU, K., BAI, C., MA, X., WANG, D., ZHAO, B., WANG, Z., LI, X. and LI, W. (2023). Cross-domain policy adaptation via value-guided data filtering. *Advances in Neural Information Processing Systems* **36** 73395–73421. [2](#), [3](#)
- YANG, W., ZHANG, L. and ZHANG, Z. (2022). Toward theoretical understandings of robust markov decision processes: Sample complexity and asymptotics. *The Annals of Statistics* **50** 3223–3248. [3](#)
- YARATS, D., FERGUS, R., LAZARIC, A. and PINTO, L. (2022). Mastering visual continuous control: Improved data-augmented reinforcement learning. In *International Conference on Learning Representations (ICLR)*. [4](#)
- YE, W., LIU, S., KURUTACH, T., ABBEEL, P. and GAO, Y. (2021). Mastering atari games with limited data. *Advances in neural information processing systems* **34** 25476–25488. [4](#), [6](#)
- YU, T., KUMAR, A., RAFAILOV, R., RAJESWARAN, A., LEVINE, S. and FINN, C. (2021). Combo: Conservative offline model-based policy optimization. *Advances in neural information processing systems* **34** 28954–28967. [2](#), [4](#)
- YU, T., THOMAS, G., YU, L., ERMON, S., ZOU, J. Y., LEVINE, S., FINN, C. and MA, T. (2020). Mopo: Model-based offline policy optimization. *Advances in Neural Information Processing Systems* **33** 14129–14142. [2](#), [4](#), [7](#), [10](#), [16](#)
- ZHAN, W., HUANG, B., HUANG, A., JIANG, N. and LEE, J. (2022). Offline reinforcement learning with realizability and single-policy concentrability. In *Conference on Learning Theory*. PMLR. [2](#)

- ZHOU, Z., ZHOU, Z., BAI, Q., QIU, L., BLANCHET, J. and GLYNN, P. (2021). Finite-sample regret bound for distributionally robust offline tabular reinforcement learning. In *International Conference on Artificial Intelligence and Statistics*. PMLR. [3](#)
- ZHU, J., XIA, Y., WU, L., DENG, J., ZHOU, W., QIN, T. and LI, H. (2020). Masked contrastive representation learning for reinforcement learning. In *Advances in Neural Information Processing Systems (NeurIPS)*. [4](#)